ADVANCED FUNCTIONAL MATERIALS

DOI: 10.1002/adfm.200800430

Selective Patterned Growth of Single-Crystal Ag–TCNQ Nanowires for Devices by Vapor–Solid Chemical Reaction**

By *Kai Xiao,** *Jing Tao, Alex A. Puretzky, Ilia N. Ivanov, Scott T. Retterer, Stephen J. Pennycook,* and *David B. Geohegan**

We report the deterministic growth of individual single-crystal organic semiconductor nanowires of silver–tetracyanoquinodimethane (Ag–TCNQ) with high yield (>90%) by a vapor–solid chemical reaction process. Ag–metal films or patterned dots deposited onto substrates serve as chemical reaction centers and are completely consumed during the growth of the individual or multiple nanowires. Selective-area electron diffraction (SAED) revealed that the Ag–TCNQ nanowires grow preferentially along the strong π–π stacking direction of Ag–TCNQ molecules. The vapor–solid chemical reaction process described here permits the growth of organic nanowires at lower temperatures than chemical vapor deposition (CVD) of inorganic nanowires. The single-crystal Ag–TCNQ nanowires are shown to act as memory switches with high on/off ratios, making them potentially useful in optical storage, ultrahigh-density nanoscale memory, and logic devices.

1. Introduction

Rapid advances in nanotechnology offer possibilities for the research of fundamental chemical and physical principles at nanometer size scales, while simultaneously developing avenues for new platform technologies such as nanoelectronics.[1] However, a fundamental issue in the assembly of complex nanomaterial architectures, such as integrated circuits, is how to address the exact locations of the component building blocks. The deterministic chemical vapor deposition (CVD) of inorganic nanowires from lithographically defined catalysis is currently a key focus for device fabrication.[2,3] However, organic nanomaterials with promising chemical/physical properties and functions are typically fabricated without catalyst assistance from the self-assembly of multifunctional molecules in solution,[4] physical vapor deposition,[5] or electrochemical templating methods.[6] The deterministic patterning of organic nanostructures has been reported only infrequently[7] and techniques similar to CVD have hardly been explored for the synthesis and patterning of organic semiconductor nanowires.

Herein, we present the selective synthesis and patterning of single-crystal Ag–TCNQ organic nanowires by a vapor–solid chemical reaction growth method. TCNQ is a good one-electron acceptor and various metal salts of TCNQ behave as charge transfer complexes which show a wide range of interesting electronic, optical, and magnetic effects.[8] Among these charge transfer compounds, Ag–TCNQ offers a particularly wide spectrum of useful properties including high structural flexibility, optical-electrical switching, and magnetism.[9] These properties make Ag–TCNQ a good candidate for applications in organic electronics, gas sensors, switches, and memory devices.[10] Nanostructured Ag–TCNQ has been previously prepared by solution processing in organic solvents, or by electrochemical and vacuum vapor reactions.[11] However, for the assembly of functional organic electronic device architectures from these materials, the growth of well-defined single-crystal Ag–TCNQ organic nanowires on selectively patterned areas is essential. In this work, long, straight, single-crystal Ag–TCNQ nanowires are synthesized by a vapor–solid chemical reaction process at 150–180 °C at atmospheric pressure. The deterministic chemical reaction approach described here allows the controllable patterned growth of either individual or multiple Ag–TCNQ nanowires from well-defined patterned sites on a surface.

[*] Dr. K. Xiao, Dr. D. B. Geohegan, Dr. I. N. Ivanov, Dr. A. A. Puretzky, Dr. S. T. Retterer
Center for Nanophase Materials Sciences
Oak Ridge National Laboratory
1 Bethel Valley Road, Oak Ridge, TN 37831-6488 (USA)
E-mail: xiaok@ornl.gov, geohegandb@ornl.gov
Dr. J. Tao, Dr. S. J. Pennycook, Dr. D. B. Geohegan
Materials Science and Technology Division
Oak Ridge National Laboratory
1 Bethel Valley Road, Oak Ridge, TN 37831-6030 (USA)
Dr. S. T. Retterer
Biosciences Division
Oak Ridge National Laboratory
1 Bethel Valley Road, Oak Ridge, TN 37831-6488 (USA)

[**] The authors gratefully acknowledge technical assistance by Pamela Fleming, and H. N. Lee for helpful discussions. This research was conducted at the Center for Nanophase Materials Sciences, which is sponsored at Oak Ridge National Laboratory by the Division of Scientific User Facilities, US Department of Energy. HRTEM and SEAD analysis (J.T., S.J.P.) funded by the Division of Materials Sciences and Engineering, Office of Basic Energy Sciences, US Department of Energy under contract DE-AC05-00OR22725 with Oak Ridge National Laboratory, managed and operated by UT-Battelle, LLC. Supporting Information is available online from Wiley InterScience or from the author.

2. Results and Discussion

Ag–TCNQ organic nanowires were grown from reactions between silver films and TCNQ vapor at 150–180 °C. A boat containing TCNQ powder was heated within a tube furnace to sublime TCNQ in an Ar atmosphere. Silver was provided either as an Ag foil or as e-beam evaporated Ag films or patterned dots deposited on substrates. Several kinds of substrates were used for nanowire growth including silicon wafers, glass and quartz slides, and flexible plastic sheets. Figure 1a shows a typical low-magnification scanning electron microscopy (SEM) image of as-synthesized Ag–TCNQ organic nanowires grown on an Ag foil. Entangled but relatively uniform Ag–TCNQ nanowires were formed on the substrate in high yield. The diameters range between 100 and 200 nm and the lengths of the nanowires can be varied between 10 and 50 μm by adjusting the growth time. A higher magnification image of a single nanowire (Fig. 1b) shows that the surfaces of the Ag–TCNQ nanowires are smooth and clean without any apparent adherent contamination. Figures 1c and d show similar SEM images of Ag–TCNQ nanowires grown from 30 nm thick Ag film deposited onto a silicon substrate. A blue layer of high-density Ag–TCNQ nanowires was visible on the Si substrate. In an energy-dispersed X-ray spectroscopy (EDS) analysis of the Ag–TCNQ nanowires, the elements of C, N, and Ag that constitute the molecules of Ag–TCNQ were clearly identified.

Figure 2a presents a SEM image of Ag–TCNQ nanowires selectively grown on a silicon substrate patterned with 25 μm^2 of 50 nm-thick Ag films. Patterned square regions were densely covered with long and straight Ag–TCNQ nanowires. In the regions without the Ag thin film coating, no wires were observed, indicating selective growth. Compared to the patterned growth of Cu–TCNQ nanowires,[12] the Ag–TCNQ nanowires here are much longer and significantly straighter. For most applications in nanoelectronics and optoelectronics, controlling the number density of the nanowires is important. This was explored through control over the size and thickness of the Ag pads. From repeated experiments with different diameters and thicknesses of the Ag dots, a threshold dot diameter $d \sim 100$–300 nm and thickness $t \sim 20$–30 nm was found to deterministically grow a single Ag–TCNQ nanowire on each patterned spot. With the patterned Ag dots $d \sim 300$ nm, $t \sim 30$–100 nm, regular arrays consisting of 1–3 nanowires at each patterned spot are consistently obtained as shown in Figure 2b and c with the lengths of about 3–10 μm. By adjusting the Ag film thickness $t \sim 20$ nm, the deterministic growth of individual nanowire with >90% yield was achieved on $d \sim 300$ nm dots, as shown in Figure 2d. The diameter of the nanowires is about 200 nm and the length is about 1 μm. This vapor–solid reaction method appears highly promising for the reliable synthesis of either individual or multiple Ag–TCNQ nanowires at specified locations, thereby enabling their integration into complex device architectures.

In order to understand the optical properties, chemical composition, and structure of the Ag–TCNQ nanowires, UV–vis absorption spectroscopy, Raman scattering, and X-ray diffraction (XRD) were used. An absorption spectrum of the nanowires is shown in Figure 3a. There are two peaks at about 375 and 634 nm in the spectral ranges of 300–440 nm and 540–760 nm, respectively, which are similar to those previously reported.[13] The peak at ca. 375 nm can be attributed to neutral Ag–TCNQ and the peaks at ca. 634 nm can be assigned to the

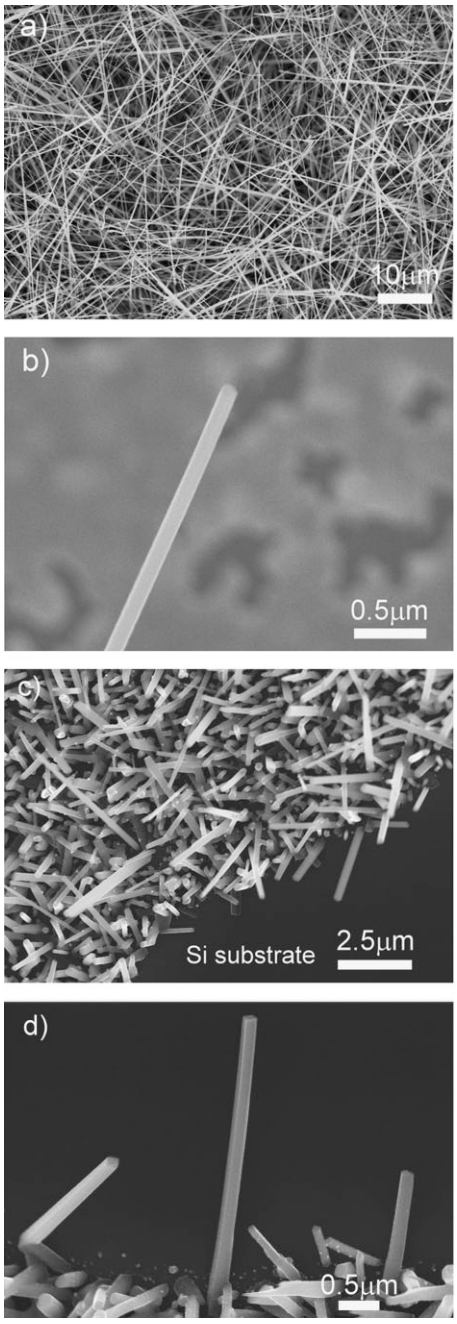

Figure 1. SEM images of Ag–TCNQ nanowires grown on a Ag foil: a) low-magnification image of a nanowire forest and b) Higher magnification image of a single nanowire tip. SEM images of Ag–TCNQ nanowires on a Si substrate (Ag film thickness: 30 nm) in c) low-magnification and d) higher magnification.

ADVANCED FUNCTIONAL MATERIALS

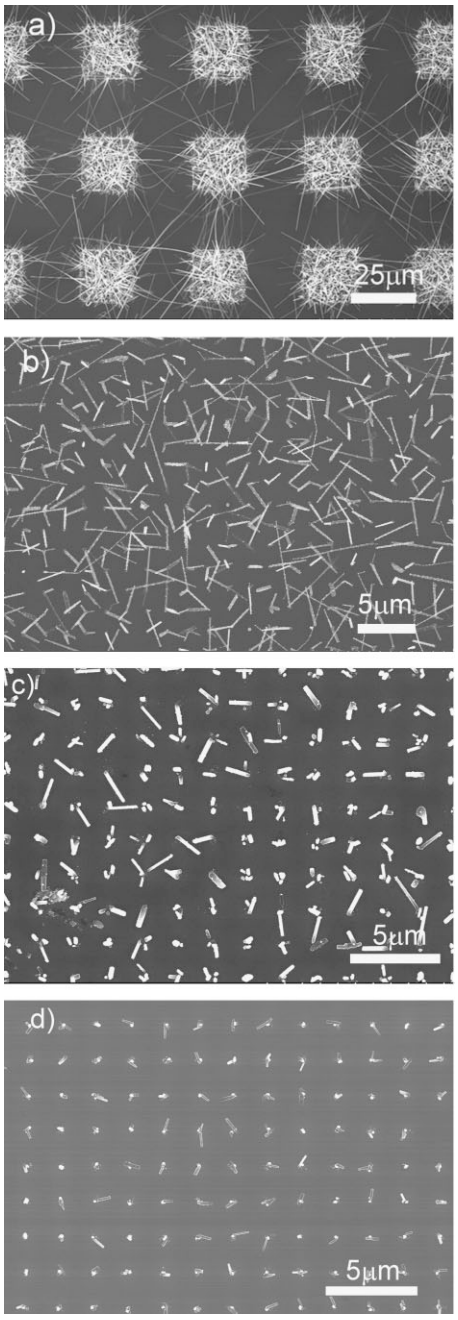

Figure 2. SEM images of patterned Ag–TCNQ nanowires on Si substrate. a) Quadrangle-patterned nanowires. Ag pads size: 25 μm and thickness: 50 nm; nanowires grown from patterned 300-nm dots of Ag with different thicknesses, b) Ag thickness: 100 nm c) Ag thickness: 30 nm, d) Ag thickness: 20 nm.

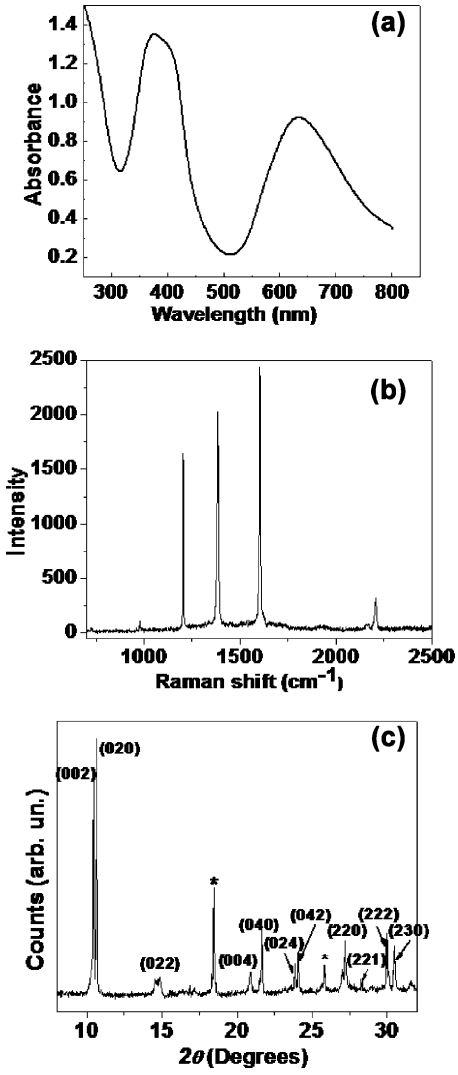

Figure 3. Characterization of the Ag–TCNQ nanowires. a) UV–Vis absorption spectrum, b) Raman spectrum, c) XRD pattern (* indicates TCNQ peak). The UV–Vis absorption spectrum was recorded at room temperature for the Ag–TCNQ nanowires grown on a glass substrate, while XRD and Raman analysis were measured using nanowire arrays grown on Si substrates.

TCNQ anion radical of Ag–TCNQ. Figure 3b shows the Raman spectrum of as-grown Ag–TCNQ nanowires, confirming that the nanowires are Ag–TCNQ via the characteristic principal vibration modes at 1204 cm^{-1} (C=CH bending), 1385 cm^{-1} (C–CN wing stretch), 1604 cm^{-1} (C=C ring stretching), and 2204 cm^{-1} (C–N stretch). However, some of the principal vibration modes of the Ag–TCNQ nanowires expected on the basis of TCNQ films at 1450 cm^{-1} (C–CN wing stretch) and 2225 cm^{-1} (C–N stretch) are, in fact, red-shifted by 65 and 21 cm^{-1}, respectively. According to previous studies, this decrease in vibrational frequency can be attributed to charge transfer between atomic Ag and free TCNQ.[14,15] The XRD patterns (Fig. 3c) taken from as-synthesized nanowires on Si substrates indicate high quality and crystalline nature of the materials. The diffraction peaks were indexed to the orthorhombic structure of Ag–TCNQ with calculated lattice constants of $a = 6.95$ Å, $b = 16.69$ Å, and $c = 17.45$ Å, which are in good agreement with the literature values for bulk Ag-TCNQ phase II.[14,16]

Figures 4a and b present low- and high-magnification TEM images, showing a portion of a typical nanowire with 100 nm

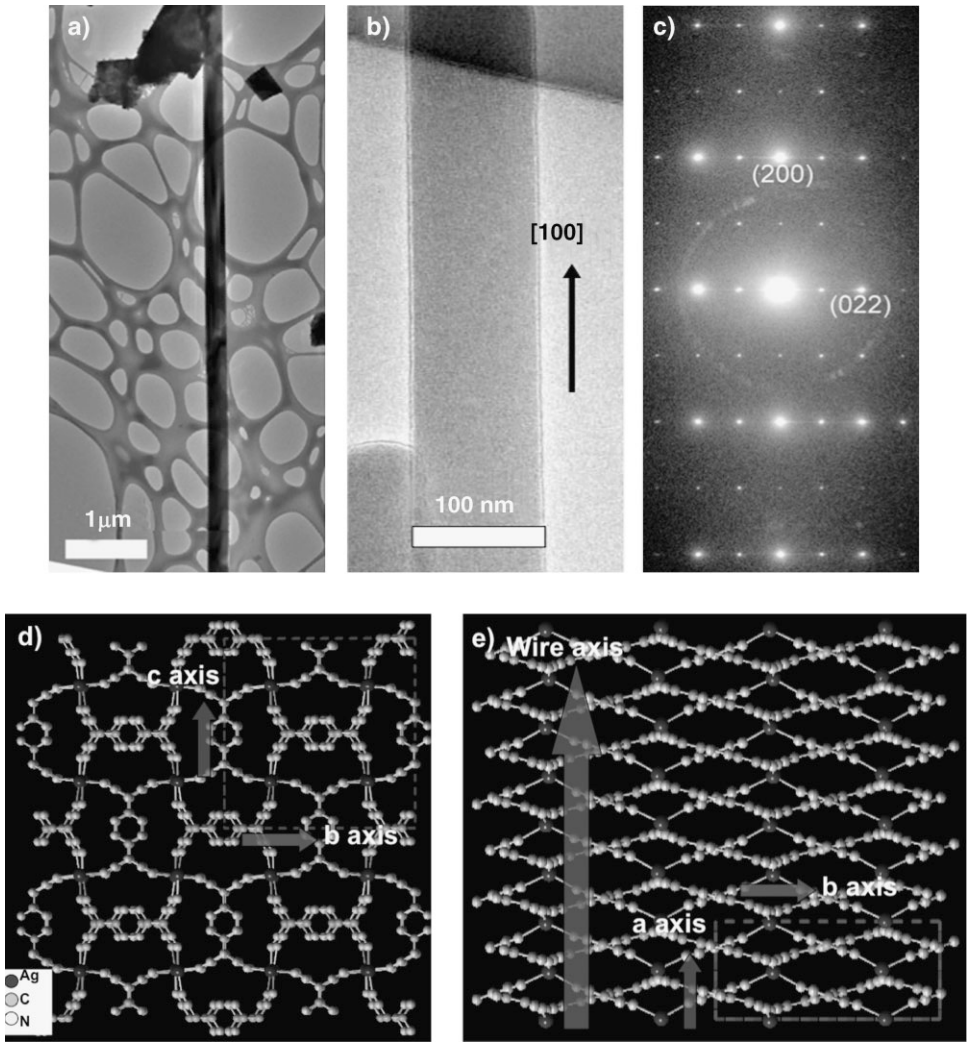

Figure 4. Morphological features and structural characterization of single-crystal Ag–TCNQ nanowires. a) Low-magnification TEM image of Ag–TCNQ nanowire placed on a holey carbon grid. b) High-magnification TEM image of a suspended Ag–TCNQ nanowire, showing preferential growth along the [100] direction. c) Selected-area electron diffraction pattern of Ag–TCNQ nanowire showing diffraction equivalent to a repeating period along the π–π stacking direction. d) Molecular structure of the (100) growth plane of Ag–TCNQ along *a*-axis. e) The derived structural model of the stacking of (100) planes along [001] direction showing the enhanced π–π overlap.

diameter. Figure 4c shows the selected-area electron diffraction (SAED) pattern obtained from the nanowire shown in Figure 4b with the electron beam perpendicular to its long axis. The highly crystalline nature of the nanowires is evident and the nanowire can be indexed as an orthorhombic Ag–TCNQ phase II crystal.[14] The pattern also shows diffraction spots equivalent to a repeating period along the π–π stacking direction with a [100] growth axis. This strongly suggests that the growth direction is along the *a*-axis of the orthorhombic Ag–TCNQ phase II structure, corresponding to stacked Ag–TCNQ molecules with large π–π overlap. Therefore, we can draw a schematic representation of the inner structure of single-crystal Ag–TCNQ nanowires with specific dimensions. The Ag atoms in the structure are coordinated to four nitrogen atoms in a highly distorted tetrahedral environment and the quinoid rings of the TCNQ units are engaged in face-to-face stacking. Adjacent TCNQ stacks have relative orientation of 90° with respect to each other and the two independent networks bring the TCNQ molecules together to give a column stack parallel to the *a*-axis with the closest distance (Figs. 4d and e). This efficient π-stacking of the TCNQ units leads to a high electrical conductivity along the nanowire. The growth process of the Ag–TCNQ nanowires was investigated by SEM and TEM. The SEM images (Supporting Information S2) show the evolution of the nanowires at different growth times.

Figures 5a and b show a schematic representation and a SEM image, respectively, of a 1D single-crystal Ag–TCNQ nanowire device patterned growth between prefabricated multilayer gap electrodes. Figure 5c shows current–voltage characteristics of a representative device based on Ag–TCNQ

ADVANCED FUNCTIONAL MATERIALS

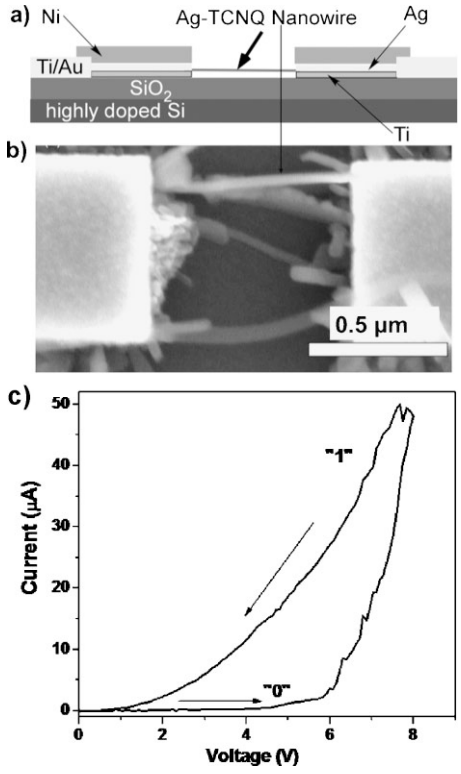

Figure 5. a) Schematic view of Ag–TCNQ nanowire patterned growth between prefabricated multilayer gap electrodes. b) SEM image of a Ag–TCNQ nanowire device. c) The typical *I–V* characteristics of the device based on the Ag–TCNQ nanowires. ''1'' and ''0'' in the curve indicate the device in the high- and low-conductivity state, respectively.

nanowire by sweeping the dc voltage applied between the electrodes. Similar electrical behavior was also observed under reversed polarity. The *I–V* curve exhibits a reversible hysteretic switching and memory behavior. As the voltage bias is increased from 0 to 8 V, the current increases monotonically at low bias until a sudden jump in current is observed at a threshold voltage (V_t) of approximately 5.5 V. The resistance changes by more than three orders of magnitude during this voltage sweep. In order to further confirm the switching behavior, devices based on an individual Ag–TCNQ nanowire were fabricated with a focused ion beam technique. The *I–V* characteristics of nanowire devices were similar to those shown in Figure 5, i.e., these devices show similar switching phenomenon (Supporting Information Fig. S3).

To confirm that the observed memory effect originated from the Ag–TCNQ nanowires, and not from deposited TCNQ molecules or crystallites, we randomly deposited TCNQ films and crystal into the same device structures at room temperature (to prevent Ag–TCNQ reaction). These TCNQ devices showed low conductivity and no switching properties (Supporting Information Fig. S4).

Such electrical switching behavior of the metal–TCNQ complex is explained as an electric field-induced reversible phase transition. This phase transition yields a partial neutral species of metal and TCNQ from metal–TCNQ and forms conduction channels in the material which substantially increase conductivity.[17] Therefore, Ag–TCNQ nanowires hold promise for applications in high density information storage as an organic electrical memory material.

3. Conclusions

Single-crystal Ag–TCNQ nanowires have been successfully synthesized and patterned by vapor–solid chemical reaction. The nanowires are predominantly phase II with efficient π-stacking of the TCNQ units leading to a high conductivity along the nanowire. The deterministic growth of single Ag–TCNQ nanowires with high yield has been demonstrated on patterned Ag dots with a threshold size of ca. 100–300 nm and thickness of ca. 20–30 nm. This capability to pattern Ag–TCNQ nanowire growth is highly desirable for future nanomanufacturing and applications, and is in particular an essential step towards in situ integration of nanowires into devices with existing technologies such as vertical transistors, memories, electron field-emitter arrays, and biosensor arrays. Reproducible *I–V* hysteresis is obtained which shows electrical switching and memory effect. The unique electrical properties of Ag–TCNQ nanowires demonstrated here are promising for applications in nanoelectronics, especially ultrahigh-density information storage.

4. Experimental

Nanowire Synthesis: In general, a 50 nm thin film of Ag was deposited with e-beam evaporation onto substrates (Si, glass, and PET foil). TCNQ powders were loaded into a ceramic boat and the substrate with Ag film was placed on the top of the boat with the Ag film-coated side facing down. The boat with substrates was placed into a 2″ quartz tube that was inserted into a tube furnace. The reaction temperature and time were precisely controlled. The temperature was increased to 150 or 180 °C and then kept at that temperature for 2 h. Finally, the temperature was decreased to room temperature. During the process, the argon gas flow rate was kept at 50–80 standard cubic centimeters per minute (sccm). During evaporation, the TCNQ vapor reacts with Ag on the substrate surface to form Ag–TCNQ nanowires.

Received: March 26, 2008
Revised: June 5, 2008
Published online: September 24, 2008

[1] a) M. S. Arnold, P. Avouris, Z. W. Pan, Z. L. Wang, *J. Phys. Chem. B* **2003**, *107*, 659. b) Y. Cui, Q. Wei, H. Park, C. M. Lieber, *Science* **2001**, *293*, 1289.

[2] a) D. Wang, H. Dai, *Angew. Chem, Int. Ed.* **2002**, *41*, 4783. b) D. Wang, R. Tu, L. Zhang, H. Dai, *Angew. Chem, Int. Ed.* **2005**, *44*, 2. c) P. Yang, H. Yan, S. Mao, R. Russo, J. Johnson, R. Saykally, N. Morris, J. Pham, R. He, H.-J. Choi, *Adv. Funct. Mater.* **2002**, *12*, 323. d) M. H. Huang, S. Mao, H. Feick, H. Yan, Y. Wu, H. K. E. Weber, R. Russo, P. Yang, *Science* **2001**, *292*, 1897.

[3] Y. Liu, H. Li, D. Tu, Z. Ji, C. Wang, Q. Tang, M. Liu, W. Hu, Y. Liu, D. Zhu, *J. Am. Chem. Soc.* **2006**, *128*, 12917.

[4] a) Y. Liu, Z. Ji, Q. Tang, L. Jiang, H. Li, M. He, W. Hu, D. Zhang, L. Jiang, X. Wang, C. Wang, Y. Liu, D. Zhu, *Adv. Mater.* **2005**, *17*, 2953. b) D. T. Bong, T. D. Clark, J. R. Granja, M. R. Ghadiri, *Angew. Chem, Int. Ed.* **2001**, *40*, 988. c) K. Balakrishnan, A. Datar, T. Naddo, J. Huang, R. Oitker, M. Yen, J. Zhao, L. Zang, *J. Am. Chem. Soc.* **2006**, *128*, 7390. d) A. K. Neufeld, A. P. O'Mullane, A. M. Bond, *J. Am. Chem. Soc.* **2005**, *127*, 13846.

[5] Y. Zhao, D. Xiao, W. Yang, A. Peng, J. Yao, *Chem. Mater.* **2006**, *18*, 2302.

[6] a) A. N. Aleshin, *Adv. Mater.* **2006**, *18*, 17. b) L. Zhi, T. Gorelik, J. Wu, U. Kolb, K. Mullen, *J. Am. Chem. Soc.* **2005**, *127*, 12792. c) H. Liu, Y. Li, L. Jiang, H. Luo, S. Xiao, H. Fang, H. Li, D. Zhu, D. Yu, J. Xu, B. Xiang, *J. Am. Chem. Soc.* **2002**, *124*, 13370.

[7] a) Q. Tang, H. Li, Y. Song, W. Xu, W. Hu, L. Jiang, Y. Liu, X. Wang, D. Zhu, *Adv. Mater.* **2006**, *18*, 3010. b) B. N. Mbenkum, E. Barrena, X. Zhang, M. Kelsch, H. Dosch, *Nano Lett.* **2006**, *6*, 2852.

[8] a) M. R. Bryce, L. C. Murphy, *Nature* **1984**, *309*, 119. b) H. Zhao, M. J. Bazile, J. R. Mascaros, K. R. Dunbar, *Angew. Chem, Int. Ed.* **2003**, *42*, 1015. c) T. Takenobu, T. Takano, M. Shiraishi, Y. Murakami, M. Ata, H. Kataura, Y. Achiba, Y. Iwasa, *Nat. Mater.* **2003**, *2*, 683. d) R. Muller, S. De Jonge, K. Myny, D. J. Wouters, J. Genoe, P. Heremans, *Solid-State Electron.* **2006**, *50*, 601.

[9] a) N. Uyeda, T. Kobayashi, K. Ishizuka, Y. Fujiyoshi, *Nature* **1980**, *285*, 95. b) E. I. Kamitsos, W. M. Risen, *Solid State Commun.* **1983**, *45*, 165. c) E. I. Kamitsos, G. C. Papavassiliou, M. A. Karakassides, *Mol. Cryst. Liq. Cryst.* **1986**, *134*, 43.

[10] Z. Y. Hua, G. R. Chen, *Vacuum* **1992**, *43*, 1019.

[11] a) C. Ye, G. Cao, F. Fang, H. Xu, X. Xing, D. Sun, G. Chen, *Micron* **2005**, *36*, 461. b) Z. Fan, X. Mo, C. Lou, Y. Yao, D. Wang, G. Chen, J.G. Lu, *IEEE Trans. Nanotechnol* **2005**, *4*, 238. c) H. Liu, Q. Zhao, Y. Li, Y. Liu, F. Lu, J. Zhuang, S. Wang, L. Jiang, D. Zhu, D. Yu, L. Chi, *J. Am. Chem. Soc.* **2005**, *127*, 1120. d) Z. Y. Fan, X. L. Mo, G. R. Chen, J. G. Lu, *Rev. Adv. Mater. Sci.* **2003**, *5*, 72. e) A. R. Harris, A. Nafady, A. P. O'Mullane, A. M. Bond, *Chem. Mater.* **2007**, *19*, 5499.

[12] a) K. Xiao, I. N. Ivanov, A. A. Puretzky, Z. Liu, D. B. Geohegan, *Adv. Mater.* **2006**, *18*, 2184. b) K. Xiao, J. Tao, Z. Pan, A. A. Puretzky, I. N. Ivanov, S. J. Pennycook, D. B. Geohegan, *Angew. Chem, Int. Ed.* **2007**, *46*, 2650.

[13] H. Gao, Z. Xue, S. Pang, *J. Phys. D: Appl. Phys.* **1996**, *29*, 1868.

[14] S. A. O'Kane, R. Clerac, H. Zhao, X. Ouyang, J. R. Galan-Mascaros, R. Heintz, K. R. Dunbar, *J. Solid State Chem.* **2000**, *152*, 159.

[15] R. S. Potember, T. O. Poehler, R. C. Benson, *Appl. Phys. Lett.* **1982**, *41*, 548.

[16] L. Shields, *J. Chem. Soc. Faraday Trans.* **1985**, *81*, 1.

[17] R. S. Potember, T. O. Poehler, D. O. Cowan, *Appl. Phys. Lett.* **1979**, *34*, 405.